

ARTICLE OPEN



LncRNA4930473A02Rik promotes cardiac hypertrophy by regulating TCF7 via sponging miR-135a in mice

Jing Ren^{1,2}, Hanping Qi^{1,2}, Chao Song¹, Lina Ba¹, Renling Liu¹, Xiang Feng¹, Lixin Wang¹, Meitian Zhang¹, Yawen Xie¹ and Hongli Sun¹

© The Author(s) 2021

Cardiac hypertrophy is a common pathological change accompanied by various cardiovascular diseases; however, its underlying mechanisms remain elusive. Mounting evidence indicates that long non-coding RNAs (lncRNAs) are novel transcripts involved in regulating multiple biological processes. However, little is known about their role in regulating cardiac hypertrophy. This study revealed a novel lncRNA4930473A02Rik (abbreviated as lncRNAA02Rik), which showed considerably increased expression in hypertrophic mouse hearts in vivo and angiotensin-II (Ang-II)-induced hypertrophic cardiomyocytes in vitro. Notably, lncRNAA02Rik knockdown partly ameliorated Ang-II induced hypertrophic cardiomyocytes in vitro and hypertrophic mouse heart function in vivo, whereas lncRNAA02Rik overexpression promoted cardiac hypertrophy in vitro. Furthermore, lncRNAA02Rik acted as a competing endogenous RNA by sponging miR-135a, while forced expression of lncRNAA02Rik could repress its activity and expression. Furthermore, forcing miR-135a overexpression exerted a significant protective effect against cardiac hypertrophy by inhibiting the activity of its downstream target TCF7, a critical member of Wnt signaling, and the protective effect could be reversed by AMO-135a. Luciferase assay showed direct interactions among lncRNAA02Rik, miR-135a, and TCF7. Altogether, our study demonstrated that lncRNAA02Rik upregulation could promote cardiac hypertrophy development via modulating miR-135a expression levels and TCF7 activity. Therefore, lncRNAA02Rik inhibition might be considered as a novel potential therapeutic strategy for cardiac hypertrophy.

Cell Death Discovery (2021)7:378; <https://doi.org/10.1038/s41420-021-00775-8>

INTRODUCTION

The heart initially develops cardiac hypertrophy under excessive stress as an adaptive response to reduce wall stress and prevent cardiac dysfunction [1, 2]. However, sustained overload causes cardiac dysfunction, eventually leading to heart failure and even sudden death [3–5]. Therefore, it is of great importance to explore and uncover the molecular mechanisms of cardiac hypertrophy.

Long non-coding RNAs (lncRNAs) are a group of transcribed RNA molecules with more than 200 nucleotides, which have no obvious protein-coding potential [6]. Previous studies have indicated that the aberrant expression of lncRNAs could be critical in multiple cardiovascular diseases [7]. For instance, Lv et al. reported that lncRNAPlscr4 controlled cardiac hypertrophy by regulating miR-214 [8]. lncRNAs have various pivotal roles with multiple mechanisms, including chromatin remodeling and RNA stability, etc [9–12]. Particularly, lncRNAs are thought to function as a “sponge” to absorb microRNAs (miRNAs) and affect post-transcriptional processing; for example, lncRNAGAS5 acts as a competing endogenous RNA (ceRNA) by sponging miR-222 [13].

MiRNAs, members of small ncRNAs, have been observed to negatively modulate gene expression primarily by base pairing to the 3'-untranslated region (UTR) of target mRNAs, leading to mRNA cleavage and translation repression [14–16]. Functionally speaking, multiple cardiovascular diseases have now been

associated with dysregulated miRNA expression [17, 18]. Our previous study indicated that miR-103 negatively affected cardiac hypertrophy via regulating Trpv3 [19]. Yuan et al. have reported that miR-21 contributed to cardiac fibrosis by targeting Smad7 [20]. The Wnt signaling pathway regulates proliferation, migration, and differentiation, and is intrinsically involved in cardiovascular development [21–23]. Previous studies have confirmed that Wnt3a and Wnt5a contribute to human cardiac fibroblasts development [24]. Similarly, TCF participates in cardio pharyngeal development in *Ciona*. [25]. Interestingly, numerous studies have indicated that ncRNAs exert a marked effect on cardiac diseases via the Wnt signaling pathway. MiR-135b could stabilize β -catenin and thus activate Wnt signaling by suppressing Apc expression [26]. Knockdown of H19 efficiently suppressed proliferation and facilitated apoptosis in ox-LDL-treated human aorta VSMCs by blocking the Wnt/ β -catenin pathway, thus alleviating intimal thickening [27]. Therefore, more research is needed to explore further associations between lncRNAs, miRNAs, and Wnt signaling in cardiac hypertrophy.

In the present study, we identified a new lncRNA, lncRNAA02Rik, which was upregulated in cardiac hypertrophy models in vivo and in vitro and appeared to function as an endogenous RNA to sponge miR-135a. Overexpression of lncRNAA02Rik and knock-down of miR-135a in myocardial cells produced the hypertrophic

¹Department of Pharmacology, Harbin Medical University-Daqing, Daqing, Heilongjiang 163319, China. ²These authors contributed equally: Jing Ren, Hanping Qi. ✉email: shlhmu@163.com

Received: 12 August 2021 Revised: 21 November 2021 Accepted: 29 November 2021
Published online: 07 December 2021

phenotype. Furthermore, TCF7 was demonstrated to be the direct target gene for miR-135a. Taken together, our study demonstrated that lncRNAA02Rik contributed to cardiac hypertrophy via sponging miR-135a and activating TCF7, a component of the Wnt signaling pathway.

RESULTS

Inhibition of lncRNAA02Rik suppressed pressure overload-induced cardiac hypertrophy

Our previous studies determined that three lncRNAs (4930473A02Rik, Gm15834, and Gm11508) were the potential risk factors in cardiac hypertrophy [28]. Here, based on the tissue expression patterns of lncRNAs in the MGI database, we found that lncRNAA02Rik was also a heart-specific expressed transcript (Fig. 1A). We then investigated the transcriptional activity of lncRNAA02Rik in the heart based on UCSC ChIP-seq tracks. As a result, lncRNAA02Rik promoter regions were occupied by abundant ChIP-seq signals, such as H3K4me3, H3K27ac, P300, and Pol2 (Fig. 1B), suggesting that lncRNAA02Rik had strong transcriptional activity. Moreover, we investigated the expression tendency of lncRNAA02Rik in heart development using ENCODE expression data. Results showed that lncRNAA02Rik was activated during the embryo period and was silenced along with heart development (Fig. 1C). Previous studies have validated that hypertrophy genes show higher expression levels during the early heart development period rather than during the adult period. Prior to expression, 3-weeks post-TAC surgery was first performed. The results showed a significantly larger proportion of heart tissue (Fig. 1D), increased cell area (Fig. 1E), and impaired cardiac function in the TAC group (Fig. 1F). Meanwhile, the increased protein and RNA levels of cardiac hypertrophy marker proteins (β -MHC and BNP) were found in TAC groups (Fig. 1G–J). Thereafter, lncRNAA02Rik expression was detected, which had been proven to be significantly enriched in hypertrophic heart tissue (Fig. 1K), suggesting that lncRNAA02Rik might be associated with the regulation of cardiac hypertrophy development.

To clarify whether the upregulation of lncRNAA02Rik contributed to cardiac hypertrophy in the mice model, we knocked down lncRNAA02Rik in mice by injecting adeno-associated virus-9 carrying a lncRNAA02Rik-specific shRNA (AAV9-shA02Rik) through the tail vein. After TAC surgery at 3 weeks, significant AAV9-shA02Rik expression was observed in cardiac tissues (Fig. 1L, M). Notably, relative to the TAC group, treatment with AAV9-shA02Rik decreased the ratios of HW/BW, LVW/BW, and LVW/TL (Fig. 1N) and reduced cardiomyocyte surface area (Fig. 1O). Furthermore, there was a decreasing trend in LVAWd and LVPWd, whereas there was an increase in LVEF and FS due to the effect of AAV9-shA02Rik, relative to the TAC group (Fig. 1P). Furthermore, AAV9-shA02Rik transfection inhibited protein upregulation and mRNA levels of cardiac hypertrophy markers BNP and β -MHC (Fig. 1Q–T). These *in vivo* results indicated that lncRNAA02Rik knockdown could inhibit cardiac hypertrophy.

Inhibition of lncRNAA02Rik prevented cardiomyocyte hypertrophy *in vitro*

To determine the role of lncRNAA02Rik in the *in vitro* model, Ang-II was used to induce cardiac hypertrophy. In order to check if we really excluded fibroblasts and myofibroblasts from cardiomyocytes, a specific marker for cardiomyocytes (cardiac troponin T) was used to stain cardiomyocytes. Results showed that the cells were cardiomyocytes stained by cardiac troponin T (Supplementary Fig. 1A). The cell area was demonstrably enlarged (Fig. 2A), and the protein and mRNA expression levels of BNP and β -MHC were significantly upregulated upon Ang-II treatment (Fig. 2B–E). Meanwhile, lncRNAA02Rik expression was detected, which was increased in the Ang-II group (Fig. 2F).

To confirm the action of lncRNAA02Rik in cardiomyocyte hypertrophy, a loss-of-function experiment was undertaken. As

displayed in Fig. 2G, siA02Rik-3 showed the most potent inhibitory effect on lncRNAA02Rik among the three siRNAs. Notably, silencing lncRNAA02Rik by siRNA targeting lncRNAA02Rik gene downregulated cardiomyocyte surface area (Fig. 2H). Meanwhile, lncRNAA02Rik knockdown significantly alleviated the protein and mRNA level of β -MHC and BNP induced by Ang-II (Fig. 2I–L). Additionally, similar results were also obtained by shA02Rik (Fig. 2M–P). The above data suggested that lncRNAA02Rik deficiency protected neonatal cardiomyocytes from hypertrophic responses. Furthermore, we employed the pcDNA3.1 plasmid to overexpress lncRNAA02Rik in cardiomyocytes. As illustrated in Fig. 2Q, lncRNAA02Rik showed a significant increase compared with the vector plasmid group. This result demonstrated that we successfully overexpressed lncRNAA02Rik in cardiomyocytes. Additionally, we observed that lncRNAA02Rik overexpression increased cell surface area (Fig. 2R) and promoted β -MHC and BNP mRNA and protein expression (Fig. 2S–V). The above results indicated that lncRNAA02Rik contributed to cardiac hypertrophy *in vitro*.

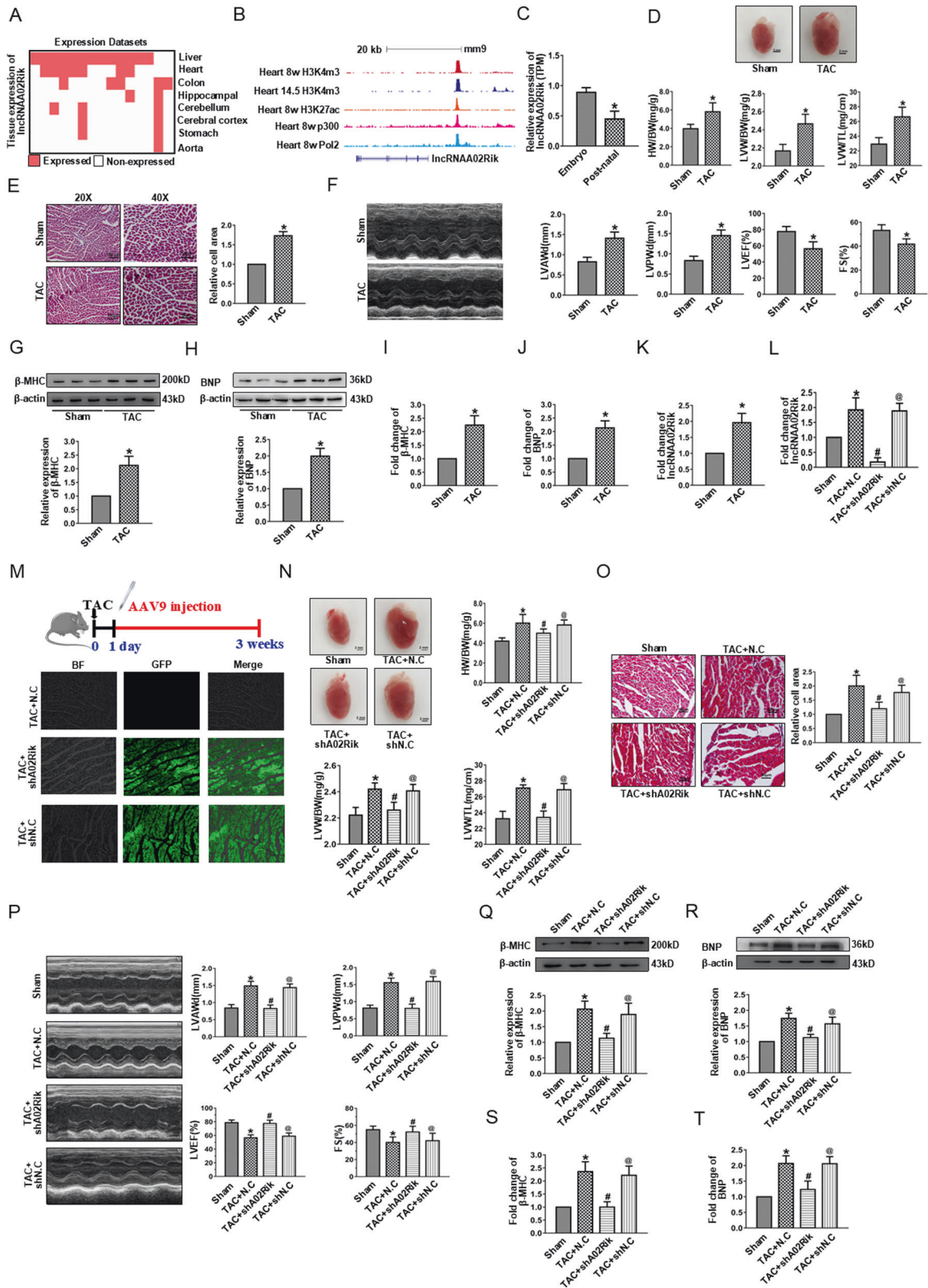
miR-135a was the potential target of lncRNAA02Rik

Evidence has shown that lncRNAs could affect miRNA function by acting as a ceRNA. Accordingly, we determined lncRNAA02Rik location using RNA fluorescence *in situ* hybridization (FISH) assays and found that most lncRNAA02Rik was located in the cytoplasm (Fig. 3A). Moreover, miR-135a was identified as one of the potential targets of lncRNAA02Rik using miRanda software and contained putative binding sites of lncRNAA02Rik (Fig. 3B). Meanwhile, miR-135a expression was differentially decreased in pressure overload-induced hypertrophic hearts (Fig. 3C). Additionally, studies have documented that miR-135a expression was altered by lncRNAA02Rik overexpression or knockdown (Fig. 3D, E). To acquire more direct evidence of the interaction between lncRNAA02Rik and miR-135a, as shown in Fig. 3F, it was observed that miR-135a decreased the luciferase activity of wild-type lncRNAA02Rik. In contrast, miR-135a did not affect mutant-type lncRNAA02Rik, indicating a direct binding relationship between lncRNAA02Rik and miR-135a.

miR-135a protected against cardiac hypertrophy by targeting TCF7

Following the above results, miR-135a expression was detected and was significantly downregulated in Ang-II-treated neonatal cardiomyocytes (Fig. 4A). These findings raised the possibility that miR-135a might be associated with the development of cardiac hypertrophy. Subsequently, we successfully overexpressed miR-135a in cardiomyocytes (Fig. 4B) to examine its effect on cardiac hypertrophy. Overexpression of miR-135a dramatically diminished the enlarged cell surface areas as well as protein and mRNA levels of BNP and β -MHC induced by Ang-II. However, these effects could be reversed by AMO-135a (Fig. 4C–G). These results suggested that miR-135a was involved in regulating of cardiac hypertrophy.

Using a bioinformatics approach, we then found that TCF7 mRNA 3'-UTRs comprised 'seed' sequences and flanking nucleotides matching miR-135a (Fig. 4H). Therefore, the impact of miR-135a on TCF7 expression using the miR-135a mimic and inhibitor was analyzed. Western blot results demonstrated that TCF7 protein expression was inhibited by overexpressing miR-135a and was promoted by AMO-135a (Fig. 4I). Similarly, the mRNA level of TCF7 change was consistent with western blot results (Fig. 4J). To investigate whether TCF7 was directly inhibited by miR-135a, we prepared luciferase constructs carrying the TCF7 3'-UTR. Results showed that the luciferase activity of wild-type TCF7 was decreased sharply by the miR-135a mimic. However, the activity of the mutant-type TCF7 was almost unchanged upon miR-135a overexpression (Fig. 4K). These data revealed a significant negative correlation between TCF7 and miR-135a and confirmed that TCF7 was the potential target gene for miR-135a.



Since TCF7 is an important component of the Wnt signaling pathway, we next sought to determine whether miR-135a could affect the activity of Wnt signaling. Ultimately, we found that the protein and mRNA levels of the downstream target gene of the

Wnt signaling pathway, c-Myc, were reduced by miR-135a overexpression, and the effect was restored by AMO-135a (Fig. 4L–M). Overall, these data indicated that miR-135a suppressed cardiac hypertrophy by directly binding to TCF7.

Fig. 1 Knockdown of *lncRNA02Rik* by shRNA attenuated cardiac hypertrophy in vivo. **A** The heatmaps of *lncRNA02Rik* expression in eight tissues. **B** *lncRNA02Rik* gene epigenomic signals in heart tissues. **C** The change in expression of *lncRNA02Rik* following heart development. **D** HW/BW heart weight to body weight ratio, LVW/BW left ventricle weight to body weight ratio, LVW/TL left ventricle weight to tibial length ratio. **E** Representative images of HE staining of mouse heart sections. Bar = 100 μ m for 20X. Bar = 50 μ m for 40X. **F** Echocardiographic parameters in mouse hearts. **G, H** Western blot results of β -MHC and BNP protein expression. **I, J** mRNA levels of β -MHC and BNP. **K** *lncRNA02Rik* expression in TAC models in vivo. **L** *lncRNA02Rik* expression by shA02Rik in vivo. **M** Protocol for AAV9-shA02Rik/AAV9-shN.C injection. **N** Cardiac morphology. Bar: 2 mm. **O** Representative images of HE staining of mouse heart sections and statistical analysis of cell area. Bar: 50 μ m. **P** Representative images of echocardiography and statistical results of echocardiographic parameters in mouse hearts. **Q, R** Western blot results of β -MHC and BNP protein expression. **S, T** mRNA levels of β -MHC and BNP. * $P < 0.05$ vs. Sham/Embryo group, # $P < 0.05$ vs. TAC + N.C group, @ $P < 0.05$ vs. TAC + shA02Rik group, $n = 6$.

TCF7, a member of Wnt signaling, promoted cardiac hypertrophy

Accumulating evidence indicates that the Wnt signaling pathway propagates the initiation and progression of cardiac diseases. However, TCF7, an important member of the Wnt signaling pathway, has an ambiguous relationship with cardiac hypertrophy. Thus, we sought to confirm whether TCF7 was involved in hypertrophic models. Elevated TCF7 protein expressions were confirmed in mouse heart tissue after TAC and in cardiomyocytes treated with Ang-II compared with sham or control group (Fig. 5A, B). Meanwhile, the protein level of c-Myc, the downstream target of TCF7, was increased consistently (Fig. 5C, D). The same changes in TCF7 and c-Myc RNA levels were also observed in vivo and in vitro groups (Fig. 5E–H). Thereafter, we used siRNA to silence TCF7 (Fig. 5I, J). Notably, we found that silencing TCF7 decreased the cell surface area (Fig. 5K), expressions of hypertrophy-related markers β -MHC (Fig. 5L), and BNP (Fig. 5M), as well as the c-Myc protein level (Fig. 5N) following Ang-II treatment. Similarly, the mRNA levels were also reduced by siTCF7 (Fig. 5O–Q). These data revealed that TCF7 acted as a component of Wnt signaling to promote the occurrence of cardiac hypertrophy.

lncRNA02Rik had a positive effect on Wnt signaling

To assess the effect of *lncRNA02Rik* on Wnt signaling, we overexpressed *lncRNA02Rik* in cardiomyocytes and found that the protein and mRNA levels of TCF7 and c-Myc were increased (Fig. 6A–D). Consistently, *lncRNA02Rik* knockdown by siRNA/shRNA led to decreased protein and mRNA levels of both TCF7 and c-Myc (Fig. 6E–L). Meanwhile, we found that *lncRNA02Rik* knockdown in TAC mice also resulted in the downregulation of the activity of TCF7 and c-Myc (Fig. 6M–P). These results indicated that *lncRNA02Rik* positively mediated Wnt signaling activity.

lncRNA02Rik contributed to cardiac hypertrophy via miR-135a/TCF7 axis

The above results demonstrated that *lncRNA02Rik* promoted cardiac hypertrophy. Moreover, miR-135a was a direct target for *lncRNA02Rik*, and it inhibited cardiac hypertrophy by suppressing TCF7-mediated Wnt pathway activity. Therefore, we hypothesized that *lncRNA02Rik* sponged miR-135a and weakened TCF7 suppression, leading to excessive Wnt pathway activity, ultimately causing cardiac hypertrophy. We then co-transfected *lncRNA02Rik* and miR-135a into cardiomyocytes and observed that miR-135a significantly altered cardiomyocyte surface area induced by *lncRNA02Rik* (Fig. 7A). Furthermore, the protein and mRNA levels of hypertrophic biomarkers (β -MHC and BNP) were lower in the co-transfected group than in the *lncRNA02Rik* only group (Fig. 7B–E), indicating that *lncRNA02Rik* promoted cardiac hypertrophy by sponged miR-135a. After co-transfecting *lncRNA02Rik* and miR-135a into cardiomyocytes, miR-135a could reverse the effect of *lncRNA02Rik* on TCF7 and c-Myc (Fig. 7F–I). Notably, the luciferase result demonstrated that miR-135a could diminish the luciferase activity of TCF7, while *lncRNA02Rik* could reverse this effect. However, *lncRNA02Rik* did not affect TCF7 activity (Fig. 7J). Collectively, these results confirmed that

lncRNA02Rik promoted cardiac hypertrophy via the miR-135a/TCF7 pathway.

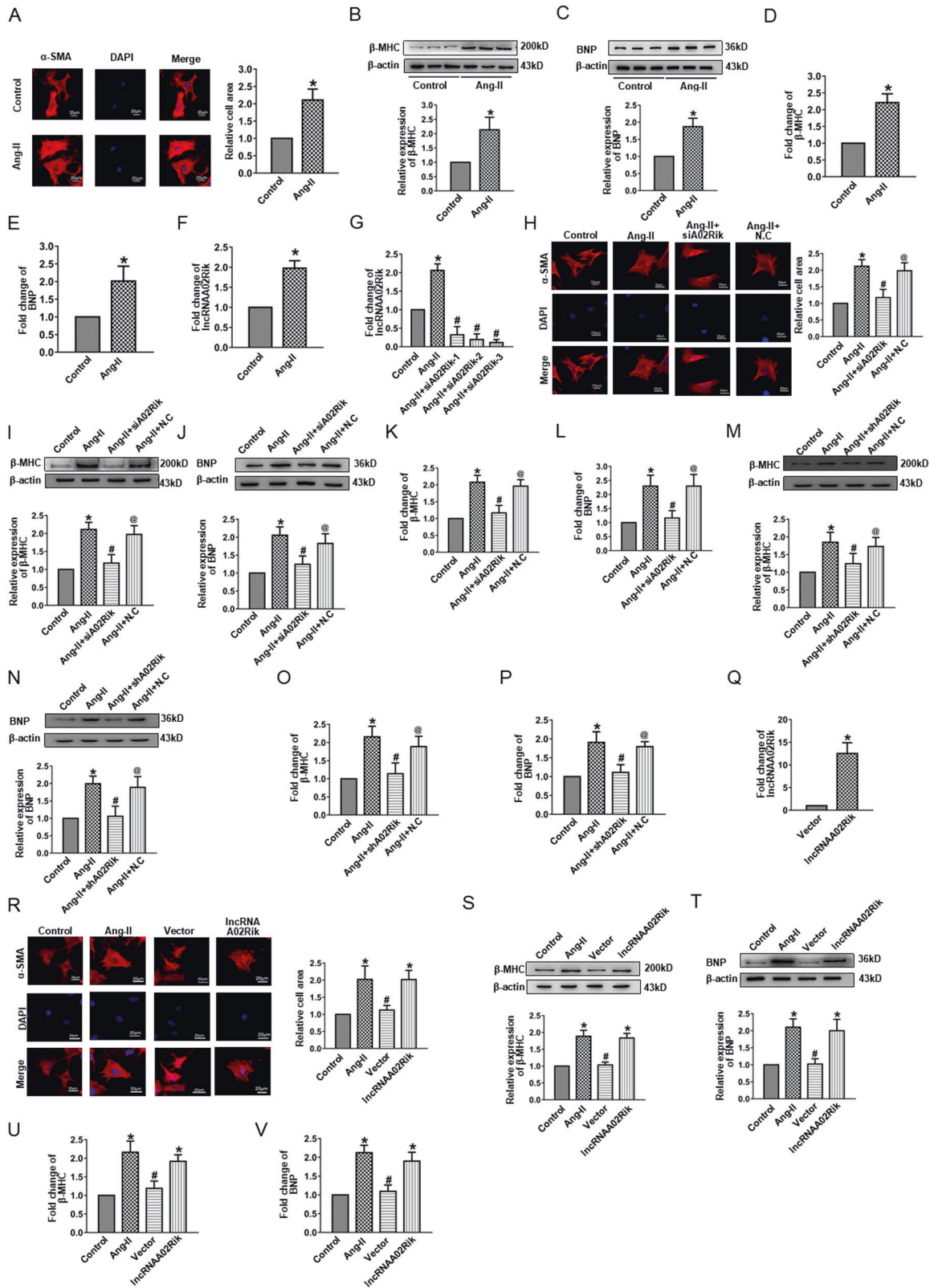
DISCUSSION AND CONCLUSION

Unlike an athlete's heart, pathological cardiac hypertrophy is triggered by pressure overload or diseases, leading to an increase in cell size rather than enhanced pumping ability. Although this problem has been extensively studied, major challenges remain.

In the present study, we reported for the first time that *lncRNA02Rik* acted as a regulator of cardiac hypertrophy. We started our research by detecting enhanced *lncRNA02Rik* expression in hypertrophic mouse hearts and cardiomyocytes. Meanwhile, this upregulation aggravated the hypertrophic phenotype both in vivo and in vitro. Furthermore, miR-135a functioned as an anti-hypertrophy miRNA by sponging *lncRNA02Rik*. In addition, TCF7 served as the target for miR-135a. Moreover, siTCF7 had a beneficial role in cardiac hypertrophic responses. Collectively, our study demonstrated that *lncRNA02Rik* exerted its hypertrophic effect through the miR-135a/TCF7 axis.

More recently, a growing number of lncRNAs have been confirmed to be responsible for cardiac diseases [29, 30]. *lncRNA02Rik*, a novel member of lncRNAs, was increased in the cardiac hypertrophy model—a finding that triggered the present study. Through gain- and loss-of-function experiments, artificial *lncRNA02Rik* overexpression in normal cardiomyocytes significantly enlarged cell area and enhanced the protein and mRNA levels of hypertrophic markers (BNP and β -MHC). In contrast, silencing *lncRNA02Rik* in hypertrophic neonatal mouse ventricular myocytes and TAC-induced hypertrophic mouse hearts markedly ameliorated hypertrophic heart function, decreased cell surface area upregulation and markedly reduced the mRNA and protein levels of BNP and β -MHC. These results indicated that *lncRNA02Rik* might have a pro-hypertrophy role, and further detailed studies were warranted to address this phenomenon.

Accumulating evidence has shown that lncRNAs could function as ceRNA to indirectly exert biological functions in various diseases, including cardiac hypertrophy [31, 32]. For example, the *lncRNAH19* functioned as a ceRNA to mediate cardiac fibrosis [33]. To explore whether *lncRNA02Rik* mediated cardiac hypertrophy by acting as ceRNA, we first conducted bioinformatics analysis using the miRanda software and determined that miR-135a contained potential binding sequences for *lncRNA02Rik*. After the prediction, RNA FISH was performed to detect the subcellular localization of *lncRNA02Rik*, and the results showed that most *lncRNA02Rik* was located in the cytoplasm. In particular, forcing the overexpression or silence of *lncRNA02Rik* could weaken or promote miR-135a expression, respectively. Additionally, co-transfection of *lncRNA02Rik* and miR-135a could reverse the pro-hypertrophic effect of *lncRNA02Rik*. At the same time, luciferase results indicated that *lncRNA02Rik* could directly bind to miR-135a. Therefore, we concluded that *lncRNA02Rik* promoted cardiac hypertrophy by competitively sponging miR-135a. Next, we investigated the effect of miR-135a on cardiac hypertrophy.



In general, miRNA-mediated gene expression and the regulation of further downstream signaling events exerted an appreciable influence on cardiac hypertrophy progression [34]. However, the role of miR-135a in cardiac hypertrophy has not been reported. In the present study, miR-135a was revealed to be

significantly inhibited, both in the TAC-induced mouse heart and cultured mouse myocardial cells following 24 h of Ang-II treatment. We then found that forcing miR-135a overexpression could significantly repress the myocardial cell area and the expression of BNP and β-MHC proteins in vitro. On the contrary,

Fig. 2 **lncRNAA02Rik contributed to cardiac hypertrophy in vitro.** **A** Immunostaining of α -SMA in cardiomyocytes. Bar: 20 μ m. **B, C** Western blot results of β -MHC and BNP protein expression. **D, E** mRNA levels of β -MHC and BNP. **F** lncRNAA02Rik expression in Ang-II-induced models in vitro. **G** Knockdown of lncRNAA02Rik by siRNAs. **H** Immunofluorescence staining of α -SMA in cardiomyocytes demonstrated that lncRNAA02Rik knockdown decreased the cell surface area. Bar: 20 μ m. **I, J** Western blot results of β -MHC and BNP protein expression in cardiomyocytes by siA02Rik. **K, L** mRNA levels of β -MHC and BNP in cardiomyocytes by siA02Rik. **M, N** β -MHC and BNP protein expression by shA02Rik in vitro. **O, P** The mRNA levels of β -MHC and BNP by shA02Rik in vitro. **Q** Forced expression of lncRNAA02Rik with a lncRNAA02Rik overexpression plasmid. **R** Immunofluorescence staining of α -SMA in cardiomyocytes demonstrated that enhanced lncRNAA02Rik expression promoted the cell surface area. Bar: 20 μ m. **S, T** Western blot results of β -MHC and BNP protein expression in cardiomyocytes by lncRNAA02Rik overexpression. **U, V** mRNA levels of β -MHC and BNP in cardiomyocytes by lncRNAA02Rik overexpression. * $P < 0.05$ vs. Control/Vector group, # $P < 0.05$ vs. Ang-II/lncRNAA02Rik group, @ $P < 0.05$ vs. Ang-II + siA02Rik/Ang-II + shA02Rik group, $n = 6$.

the anti-miR-135a significantly enhanced their expressions in cardiac hypertrophy. Furthermore, to identify the direct target for miR-135a, TargetScan software was used to predict the downstream genes of miR-135a. We found that TCF7 was the most likely target gene for the miR-135a. The luciferase activity and TCF7 protein expression results confirmed that TCF7, a central component of the Wnt signaling pathway whose downstream target was c-Myc, was a direct target for miR-135a. In this study, TCF7 and c-Myc levels were significantly increased in TAC-induced mouse hearts and Ang-II-treated cultured mouse myocardial cells. Furthermore, silencing TCF7 could significantly diminish the cardiomyocyte area and decrease BNP and β -MHC protein levels and mRNA expression. Taken together, the data suggested that the miR-135a protected against cardiac hypertrophy by inhibiting TCF7 expression and then blocking the Wnt signaling pathway. Moreover, the luciferase experiment demonstrated that lncRNAA02Rik sponging miR-135a could abolish the derogation of the target gene TCF7 by miR-135a. Furthermore, co-transfection of lncRNAA02Rik and miR-135a could ameliorate the pro-hypertrophic effect of lncRNAA02Rik. Therefore, lncRNAA02Rik promoted cardiac hypertrophy through the miR-135a/TCF7 signaling pathway.

Taken together, our study revealed that lncRNAA02Rik, as a critical pro-hypertrophic lncRNA, could promote cardiac hypertrophy via the miR-135a/TCF7 signaling pathway, implying that lncRNAA02Rik could be considered as a novel therapeutic target. Accordingly, siA02Rik or other forms of the lncRNAA02Rik inhibitor could be developed into novel therapeutic agents for treating cardiac hypertrophy.

MATERIALS AND METHODS

Bioinformatics analysis of lncRNAA02Rik

To observe the expression patterns of lncRNAA02Rik in mouse hearts and other tissues, we first downloaded the expression profile of lncRNAA02Rik from the MGI database (<http://www.informatics.jax.org/>). Then, we classified the expression data into "expressed" or "non-expressed" groups based on the expression thresholds of the MGI database and exhibited these in a heatmap. We also observed the transcriptional activity of lncRNAA02Rik in the heart. Briefly, we downloaded ChIP-seq data (histone: H3K4me3 and H3K27ac; Co-factor: P300 and Pol2) of the heart from the UCSC table browsers (<http://genome.ucsc.edu/>), and data visualization was conducted using the IGV browser with mm9 as the reference genome. In addition, we also downloaded heart development expression data from the ENCODE database (<https://www.encodeproject.org/>).

Cardiac hypertrophy induced by pressure overload in vivo

All the animal experimental procedures were performed following the Guide for the Care and Use of Laboratory Animals published by the US NIH (publication, 8th Edition, 2011), and approved by the Experimental Animal Ethics Committee of Harbin Medical University-Daqing. Briefly, C57BL/6 mice of 22–24 g (8–10 weeks old) were anesthetized by intraperitoneal injection with sodium pentobarbital (30 mg/kg, i.p.). To visualize the aortic arch, under aseptic conditions, a 2–3 mm longitudinal incision was performed in the proximal sternum. An overlaying blunted 27-gauge needle and a 6-0 silk suture were then used for transverse aorta constriction; the needle was quickly removed to make the constriction. Mice received meloxicam (1.6 mg/kg, s.c.) immediately after surgery and

again 12 h postoperatively. Mice were kept warm under a heat lamp and monitored until they were awake and ambulatory, at which time they were returned to their home cages. After 3 weeks, echocardiography analysis was conducted to evaluate cardiac function, including left ventricular posterior wall end-diastolic diameter (LVPWd), left ventricular anterior wall end-diastolic diameter (LVAWd), left ventricular ejection fraction (LVEF), and fractional shortening (FS). Finally, the mice were sacrificed to examine the heart weight (HW), body weight (BW), left ventricular weight (LVW), and tibial length (TL) [8].

Neonatal mouse cardiomyocyte culture

Neonatal mouse cardiomyocytes were harvested as previous study [35–37]. Briefly, hearts were obtained from C57BL/6 mice (1 to 3 days old) and repeatedly rinsed with ice-cold phosphate-buffered saline solution. Thereafter, ventricular tissues were minced with scissors and enzymatically dissociated using 0.25% trypsin at 37 °C, and pooled cell suspensions were centrifuged and then resuspended in Dulbecco's modified Eagle's medium with 10% fetal bovine serum. The suspension was coated on the culture bottle for 90 min, allowing the fibroblasts to attach preferentially to the bottom of the bottle. Weak-adherent and non-adherent cells were regarded as cardiomyocytes and transferred to a new culture bottle for further experiments, and 0.01 nmol/L 5-Bromo-2-deoxydriune was added to exclude the cardiac fibroblasts. Finally, to induce hypertrophy, angiotensin-II (Ang-II) was added to the cardiomyocyte at a concentration of 100 nmol/L for 24 h.

Western blotting

Myocardial cells and heart tissue were lysed in cold radioimmunoprecipitation assay buffer. A bicinchoninic acid protein assay was used to quantify protein samples. Identical quantities of protein samples were separated by SDS-PAGE and transferred onto a nitrocellulose membrane. Thereafter, the membrane was blocked with 5% skim milk at room temperature for 2 h, followed by incubation with the specific primary antibody at 4 °C overnight: anti-BNP antibody (1:1,000 dilution, sc-271185, Santa Cruz), anti- β -MHC antibody (1:2,000 dilution, SAB2106550, Sigma), anti-TCF7 antibody (1:300 dilution, A01315-2, Boster), anti-c-Myc antibody (1:300 dilution, BM4042, Boster), and anti- β -actin antibody (1:2000 dilution, TA-09, ZSGB-BIO). β -actin was used as a loading control. After washing thrice for 10 min each time in Tris-buffered saline with Tween (TBST), the membrane was incubated with the secondary antibody at room temperature for 1 h and washed again in TBST. Subsequently, the bands were scanned using an Odyssey Imaging System (LI-COR Biosciences, Lincoln, NE, USA).

Hematoxylin-eosin (HE) staining

After anesthesia, the hearts were quickly removed and immersed in 4% paraformaldehyde solution for 24 h. Next, the tissue was cut into 5- μ m-thick cross-sectional slices. These slices were stained with HE to evaluate histopathology. Photographs were captured using an Olympus BX60 microscope (Olympus Optical, Tokyo, Japan), and cell areas were calculated using image analysis software (Image-Pro Plus 6.0 software).

Immunofluorescence staining

The cells on coverslips were fixed with 4% paraformaldehyde for 15 min and permeabilized with 0.2% Triton X-100 for 15 min. Thereafter, goat serum was used to block cells for 30 min at room temperature. α -Smooth muscle actin (α -SMA) antibody (1:200 dilution, #19245, Cell Signaling) and cardiac troponin T antibody (1:100 dilution, A4914, ABclonal) were added, followed by incubation at 4 °C overnight [38, 39]. The second antibody was then added, followed by incubation in the dark for 1 h. The slides were observed under a fluorescence microscope (Leica, Heidelberg, Germany),

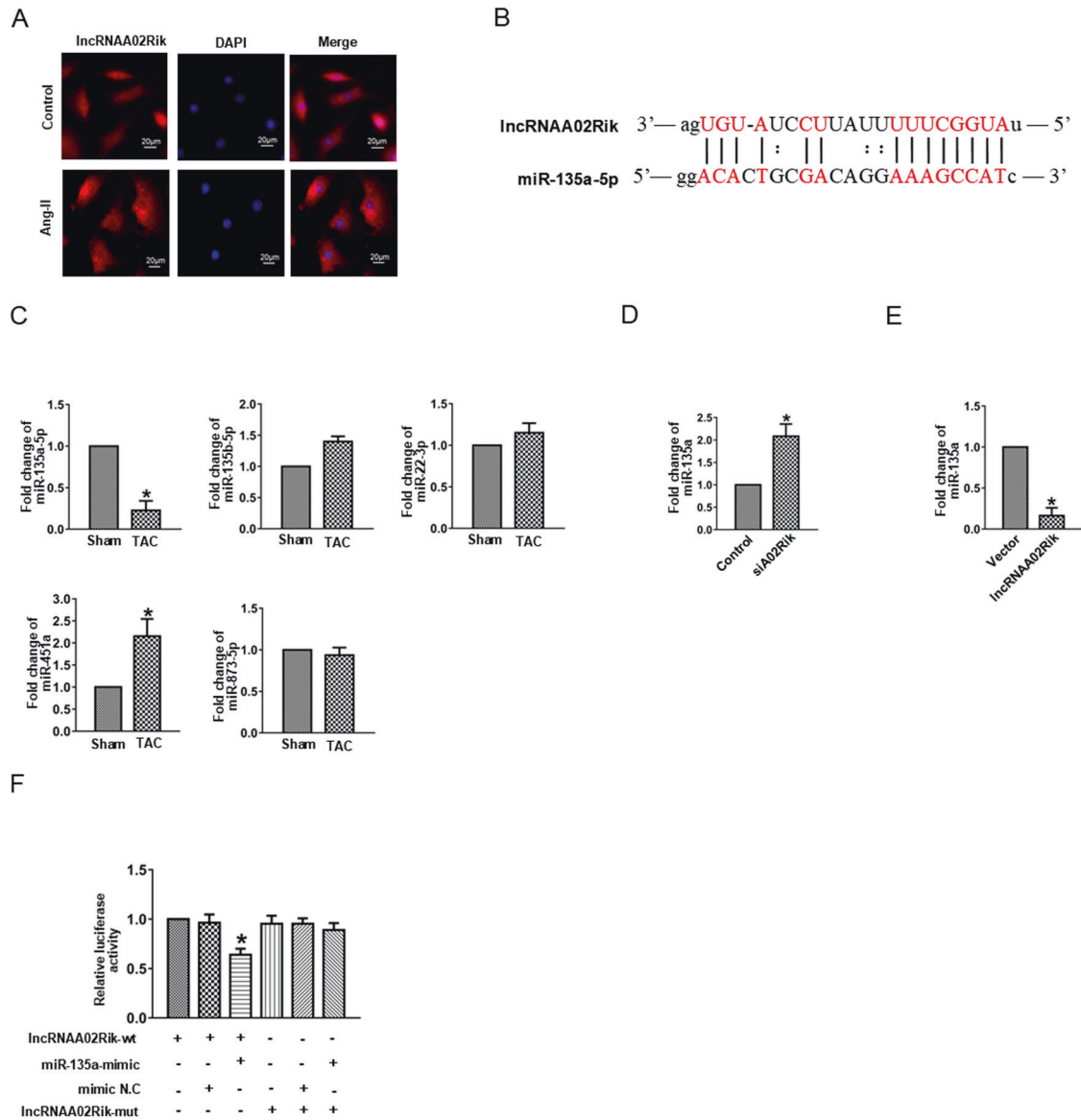


Fig. 3 miR-135a was the target of lncRNA02Rik. **A** Subcellular localization detection of lncRNA02Rik. Bar: 20 μ m. **B** The binding sites between lncRNA02Rik and miR-135a were determined using miRanda software. **C** Relative expression of miR-135a-5p, miR-135b-5p, miR-22-3p, miR-451a, and miR-873-5p. **D** Expression level of miR-135a in cardiomyocytes transfected with siA02Rik. **E** Expression level of miR-135a in cardiomyocytes transfected with the lncRNA02Rik plasmid. * $P < 0.05$ vs. Control/Vector/Sham group, $n = 6$. **F** Luciferase reporter gene assay of lncRNA02Rik and miR-135a. * $P < 0.05$ vs. lncRNA02Rik-wt group, $n = 3$.

and cell areas were calculated using image analysis software (Image-Pro Plus 6.0 software).

Quantitative real-time polymerase chain reaction (qPCR)

TRIzol was used to extract the total RNA from the heart tissues of mice or cultured cells following the manufacturer's protocol. qPCR was performed using a LightCycler[®] 480 system (Roche, Basel, Switzerland) with SYBR Green I Master Mix (Roche). Each reaction system consisted of 20 ng cDNA. After a 40-cycle reaction, amplification was used to calculate the CT value (Δ CT) of target genes and the difference between the Δ CT of those genes and the 18 s, U6, or GAPDH gene. In addition, the $2^{-\Delta\Delta CT}$ equation was used to determine the relative amount of lncRNA, miRNA, or mRNA in specific target genes.

The sequences of primers were as follows:

lncRNA02Rik:

Forward: TGCCATTCTGAGGGTTCTG

Reverse: ACGATTGAGGACTTCTGGC

miR-135a-5p reverse transcriptase primer:

CTCAACTGGTGTCTGGAGTCGGCAATTCAGTTGAGTCACATAG

miR-135a-5p:

Forward: CTGGTAGGTATGGCTTTTATTC

Reverse: TCAACTGGTGTCTGGAGTC

miR-22-3p reverse transcriptase primer:

CTCAACTGGTGTCTGGAGTCGGCAATTCAGTTGAGACAGTTCT

miR-22-3p:

Forward: ACACTCCAGCTGGGAAGCTGCCAGTTGAAG

Reverse: GGTCGTCGGAGTCGGCAA

miR-135b-5p reverse transcriptase primer:

GTCGTATCCAGTGCCTGTCGTGGAGTCGGCAATTCAGTGGATACGACTCA-CAT

miR-135b-5p:

Forward: GGATGGCTTTTCATTCCT

Reverse: CAGTGCCTGTCGTGGAGT

miR-451a reverse transcriptase primer:

GTCGTATCCAGTGCAGGGTCCGAGGTATTCGACTGGATACGACAGCAA

miR-451a:

Forward: ACACTCCAGCTGGGAAACCGTTACCATTACT

Reverse: CTGGTGTCTGGAGTCGGCAA

miR-873-5p reverse transcriptase primer:

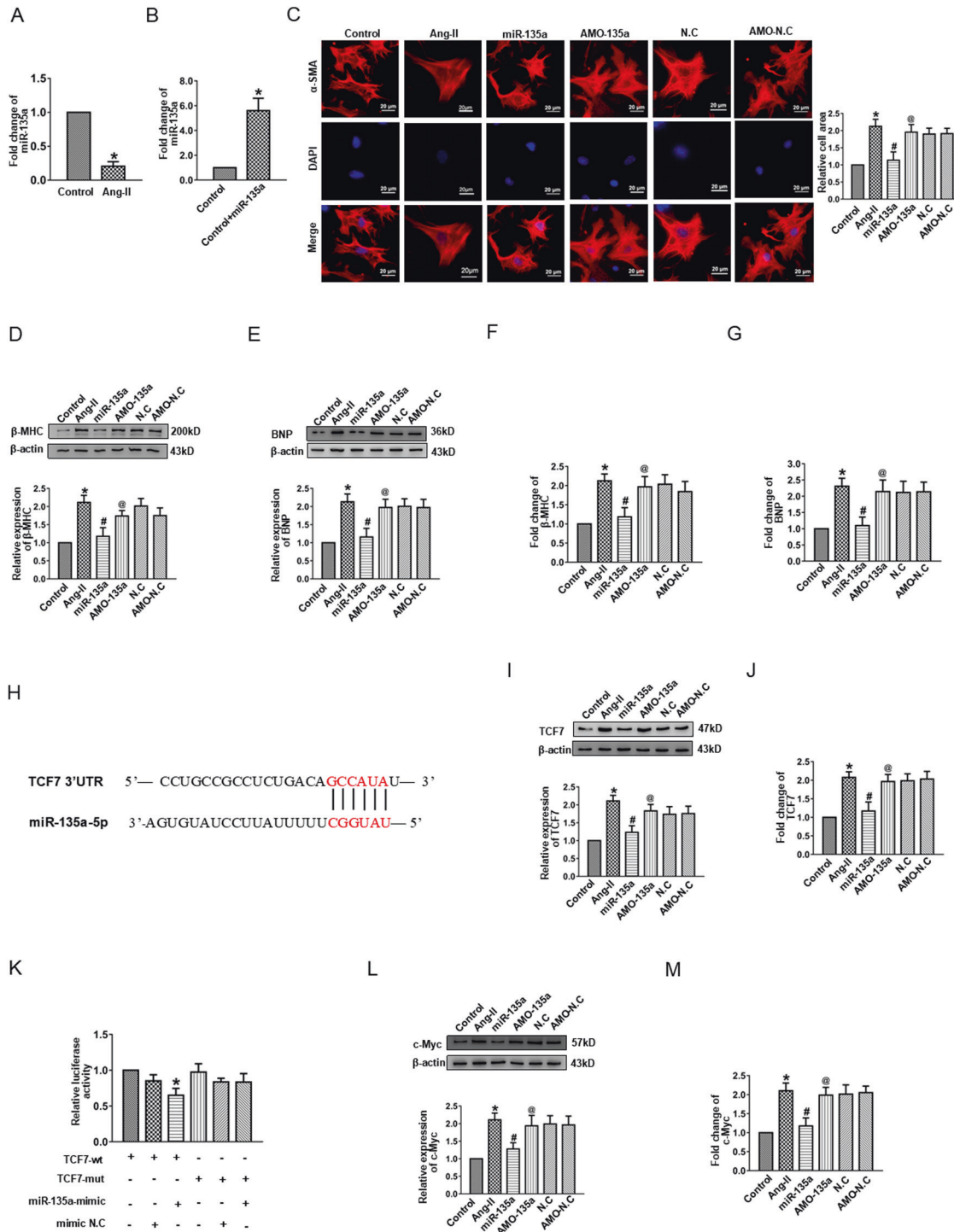


Fig. 4 miR-135a inhibited cardiac hypertrophy by targeting TCF7. **A** The expressions of miR-135a in cardiac hypertrophy models in vitro. **B** Expression level of miR-135a in cardiomyocytes transfected with scramble or miR-135a mimics. **C** Immunostaining of α-SMA in cardiomyocytes transfected with miR-135a mimics. Bar: 20 μm. **D**, **E** Western blot results of β-MHC and BNP protein expression in cardiomyocytes transfected with miR-135a mimics. **F**, **G** mRNA levels of β-MHC and BNP in cardiomyocytes transfected with miR-135a mimics. **H** The binding sites of miR-135a and TCF7 were determined using TargetScan software. **I** Western blot results of TCF7 protein expression by miR-135a mimics. **J** The mRNA level of TCF7 in cardiomyocytes by miR-135a mimics. **K** Luciferase reporter activities of chimeric vectors carrying the luciferase gene and a fragment of TCF7 3'-UTR containing the binding sites of miR-135a. **P* < 0.05 vs. TCF7-wt group, *n* = 3. **L** Western blot results of c-Myc protein expression by miR-135a mimics. **M** The mRNA level of c-Myc in cardiomyocytes by miR-135a mimics. **P* < 0.05 vs. Control group, #*P* < 0.05 vs. Ang-II group, @*P* < 0.05 vs. miR-135a group, *n* = 6.

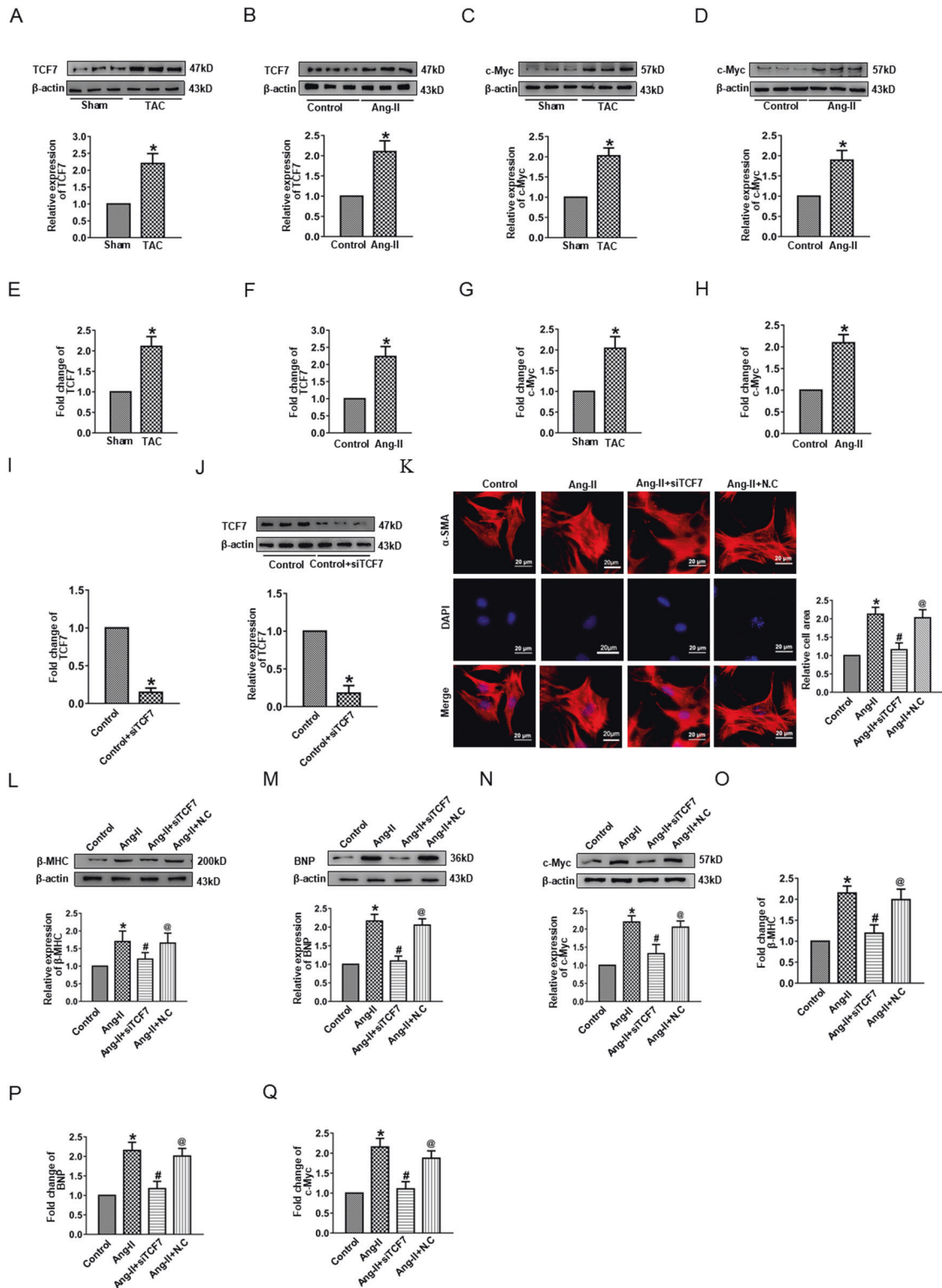


Fig. 5 The effect of TCF7 on cardiac hypertrophy. **A, B** Western blot results of TCF7 protein expression. **C, D** Western blot results of c-Myc protein expression. **E, F** mRNA level of TCF7. **G, H** mRNA level of c-Myc. **I** mRNA level of TCF7 in cardiomyocytes by siTCF7. **J** TCF7 protein expression in cardiomyocytes by siTCF7. **K** Immunostaining of α -SMA in cardiomyocytes transfected with siTCF7. Bar: 20 μ m. **L, M** Western blot results of β -MHC and BNP protein expression in cardiomyocytes by siTCF7. **N** Western blot results of c-Myc protein expression in cardiomyocytes by siTCF7. **O, P** mRNA levels of β -MHC and BNP in cardiomyocytes by siTCF7. **Q** mRNA level of c-Myc in cardiomyocytes by siTCF7. * P < 0.05 vs. Sham/Control group, # P < 0.05 vs. Ang-II group, @ P < 0.05 vs. Ang-II + siTCF7 group, n = 6.

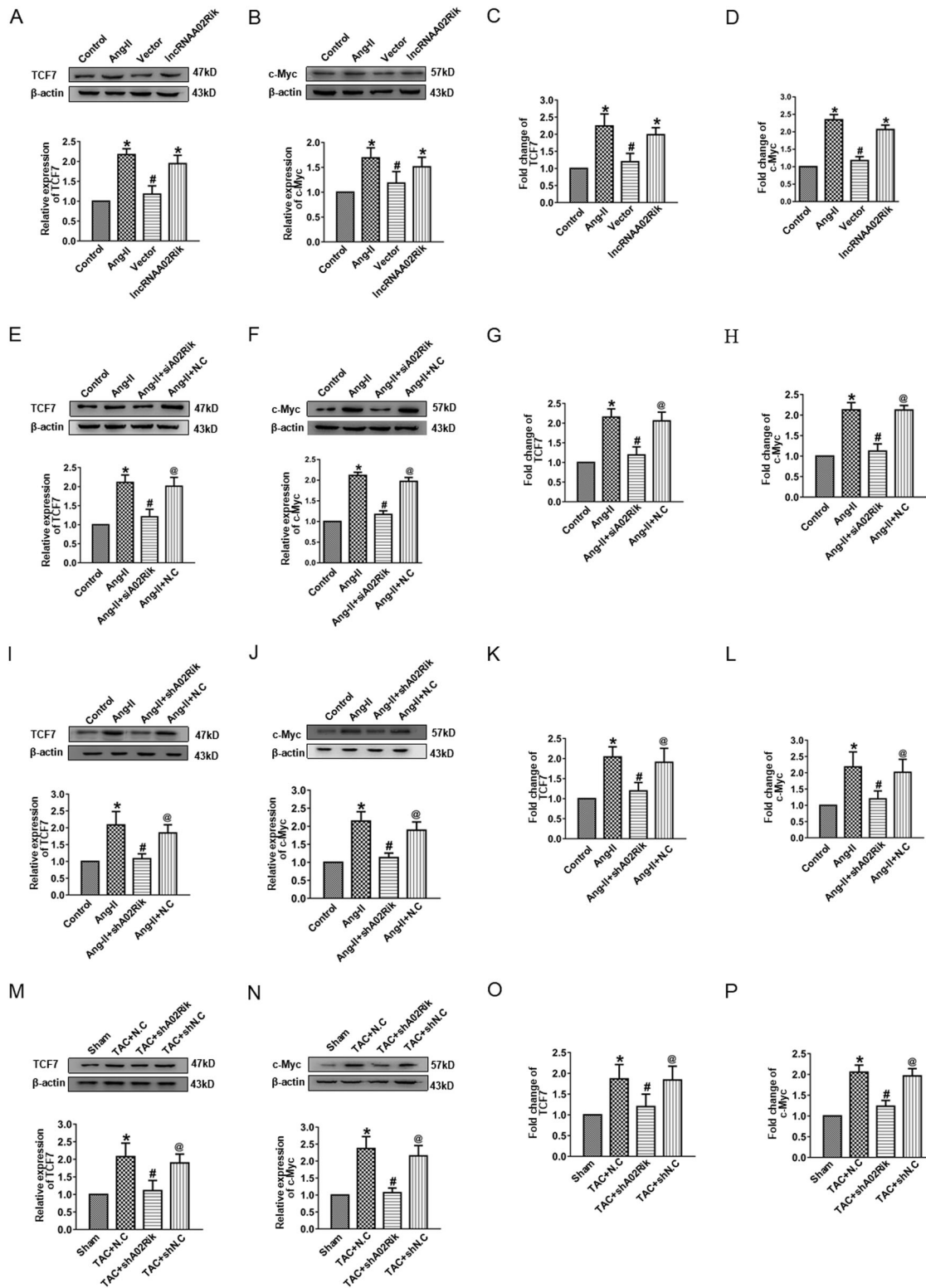


Fig. 6 The effect of lncRNA02Rik on Wnt signaling. **A, B** Western blot results of TCF7 and c-Myc protein expression by lncRNA02Rik overexpression. **C, D** mRNA levels of TCF7 and c-Myc by lncRNA02Rik overexpression. **E, F** Western blot results of TCF7 and c-Myc protein expression by siA02Rik. **G, H** mRNA levels of TCF7 and c-Myc by siA02Rik. **I, J** Western blot results of TCF7 and c-Myc protein expression by siA02Rik in vitro. **K, L** mRNA levels of TCF7 and c-Myc by siA02Rik in vitro. **M, N** Western blot results of TCF7 and c-Myc protein expression by siA02Rik in vivo. **O, P** mRNA levels of TCF7 and c-Myc by siA02Rik in vivo. * $P < 0.05$ vs. Sham/Control group, # $P < 0.05$ vs. TAC + N.C./Ang-II/lncRNA02Rik group, @ $P < 0.05$ vs. Ang-II + siA02Rik/Ang-II + siA02Rik/TAC + siA02Rik group, $n = 6$.

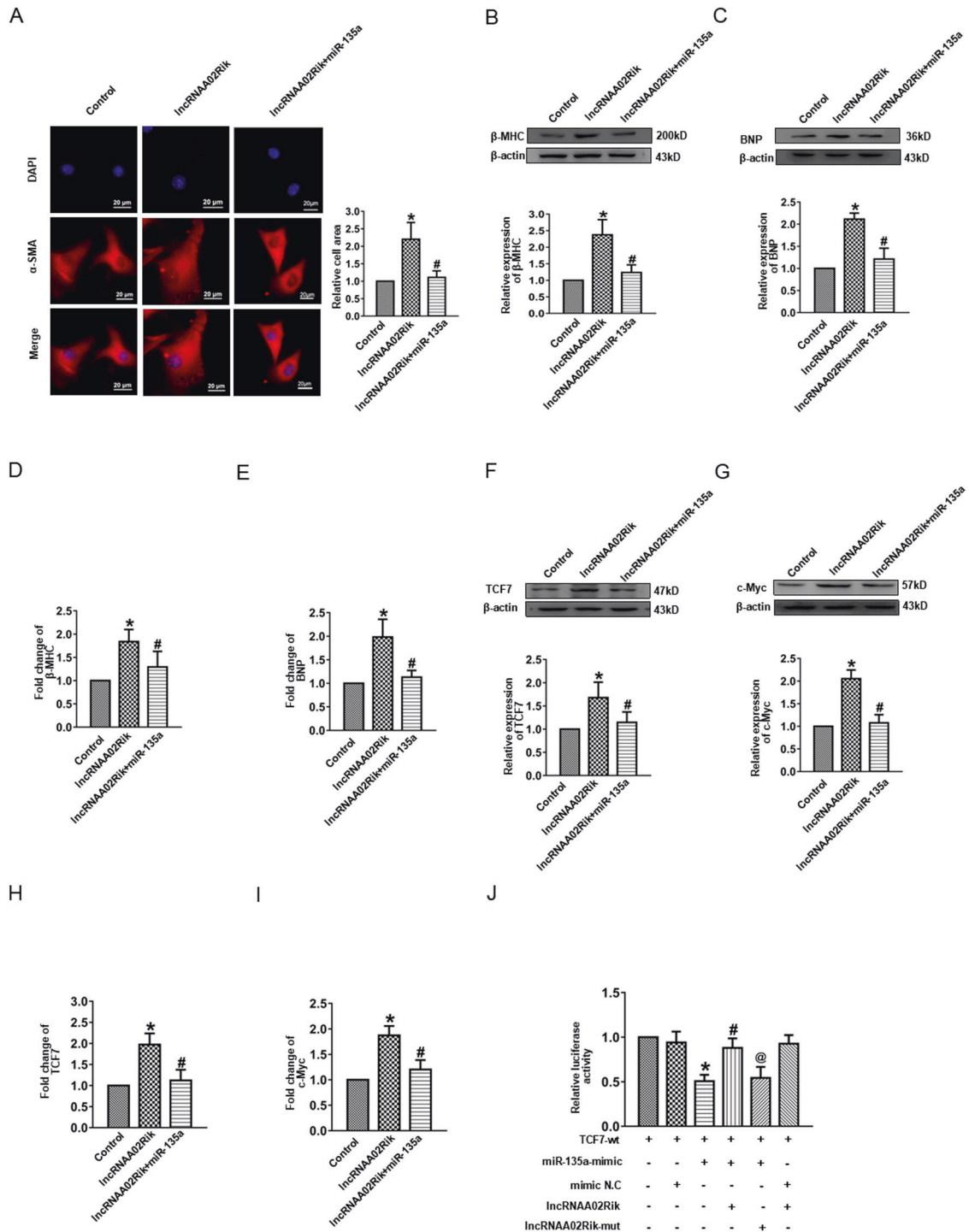


Fig. 7 The relationship between lncRNA02Rik, miR-135a, and TCF7. **A** Immunostaining of α -SMA by co-transfection of lncRNA02Rik and miR-135a in cardiomyocytes. **B, C** Western blot results of β -MHC and BNP protein expression in cardiomyocytes by co-transfection. **D, E** mRNA levels of β -MHC and BNP in cardiomyocytes by co-transfection. **F, G** Western blot results of TCF7 and c-Myc protein expression in cardiomyocytes by co-transfection. **H, I** mRNA levels of TCF7 and c-Myc in cardiomyocytes by co-transfection. **J** The luciferase reporter gene was used to validate the regulatory interactions among lncRNA02Rik, miR-135a, and TCF7. * $P < 0.05$ vs. Control group, # $P < 0.05$ vs. lncRNA02Rik group, $n = 6$. **J** The luciferase reporter gene was used to validate the regulatory interactions among lncRNA02Rik, miR-135a, and TCF7. * $P < 0.05$ vs. TCF7-wt group, # $P < 0.05$ vs. TCF7-wt+miR-135a-mimic group, @ $P < 0.05$ vs. TCF7-wt + miR-135a-mimic + lncRNA02Rik group, $n = 3$.

GTCGTATCCAGTGCAGGGTCCGAGGTATTGCACTGGATACGACGTCAAA
miR-873-5p:
Forward: GCAGGAAGTGTGAG
Reverse: GTGCAGGGTCCGAGGT
 β -MHC:
Forward: TATCGATGACCTGGAGCTGA

Reverse: AGTATTGACCTTGTCTTCTC
BNP:
Forward: ACAGAAGCTGCTGGAGCTGA
Reverse: CCGATCCGGTCTATCTTGTG
GAPDH:
Forward: ACAGCAACAGGGTGGTGGAC

Reverse: TTTGAGGGTGCAGCGAACTT
 TCF7:
 Forward: TCGGGTGTGGAGAAGACTGGCAT
 Reverse: CTGGCTGATGTCCGCTGGTG
 c-Myc:
 Forward: CGTTGGAACCCCGCAGACA
 Reverse: GATATCCTACTGGGCGCGG
 U6:
 Forward: CGTTCACGAATTTGCGTGTTCAT
 Reverse: GCTTCGGCAGCATATACTAAAAAT
 18s:
 Forward: TAGAGGGACAAGTGGCGTTC
 Reverse: CGCTGAGCCAGTCAGTGT

Knockdown of lncRNA02Rik by siRNA and shRNA

lncRNA02Rik-specific siRNA (siA02Rik) and shRNA (shA02Rik) were commercially manufactured by GenePharma (Shanghai, China) as well as IBSBIO Tech. According to the manufacturer's protocol, the cells were transfected with siA02Rik/shA02Rik (1 µg/mL) and X-tremeGENE Transfection Reagent (Roche, Penzberg, Germany) with 300 µl Serum-free Medium for 5 min. Subsequently, the two reagents were mixed and combined for 18 min at room temperature, after which the mixture was put into cells for 6 h at 37 °C. Thereafter, cardiomyocytes were maintained in the culture medium for 48 h until subsequent experiments.

The sequences of siA02Rik-1 were Forward: CAGAGACUGUCAAGAGU CAGA, Reverse: UGACUCUUGACAGUCUCUGUA; siA02Rik-2 sequences were Forward: GAAUGAUCACUCUGUUAAAUU, Reverse: UUUAAACAGAGUGAU CAUUGCA; siA02Rik-3 sequences were Forward: GGACUGUGCUCAAGGCA CAGA, Reverse: UGUGCCUUGAGCACAGUCCUG; the sequences of siRNA negative control (siN.C) were Forward: UUCUCCCAACGUGUCACGUTT, Reverse: ACGUGACACGUUCGGAGAATT; shA02Rik sequences were GGACT GTGCTCAAGGCACAGA; the sequences of shRNA negative control (shN.C) were CCTAAGGTTAAGTCGCCCTCG.

Cells were separated into four groups: (1) Control group; (2) Ang-II group: cells were treated with 100 nmol/L Ang-II for 24 h; (3) Ang-II + siA02Rik/Ang-II + shA02Rik group: cells were transfected with siA02Rik/shA02Rik for 24 h then removed it and treated with 100 nmol/L Ang-II for 24 h; (4) N.C group: cells were transfected with siN.C/shN.C for 24 h then removed it and treated with 100 nmol/L Ang-II for 24 h.

Overexpression of lncRNA02Rik by plasmid

lncRNA02Rik cDNA was combined with the pcDNA3.1 vector. An empty vector was regarded as the negative control. Similar to siRNA transfection, plasmid vectors were transfected into cells at a 2.5 mg/L concentration.

Cells were separated into four groups: (1) Control group; (2) lncRNA02Rik group: lncRNA02Rik plasmid was transfected into cells for 24 h; (3) Vector group: pcDNA3.1 empty vector was transfected into cells for 24 h; (4) Ang-II group.

miRNA transfection

The mimics and inhibitors of miR-135a-5p were synthesized by GenePharma and the protocol was the same as that for siRNA transfection.

The sequences of miR-135a-5p mimics were Forward: UAUGGCUUUUUUUAUCCUAUGUGA, Reverse: ACAUAGGAAUAAAAGCCAUUUU; miR-135a-5p inhibitor (AMO-miR-135a-5p) sequences were UCACAUGGAAUAAAAGCCAUU; negative control (N.C) sequences were Forward: UUCUCCGAAACGUGUCACGUTT, Reverse: ACGUGACACGUUCGGAGAATT; negative control inhibitor (AMO-N.C) sequences were CAGUACUUUUUGUG UAGUACAA.

Cells were separated into six groups: (1) Control group; (2) Ang-II group; (3) Ang-II + miR-135a group: cells were treated with Ang-II for 24 h then removed and transfected with miR-135a-5p mimics for 24 h; (4) Ang-II + miR-135a+AMO-135a group: cells were treated with Ang-II for 24 h then removed it and transfected with miR-135a-5p mimics and AMO-miR-135a-5p for 24 h; (5) Ang-II + N.C group: cells were treated with Ang-II for 24 h then removed it and transfected with the negative control for 24 h; (6) Ang-II + AMO-N.C group: cells were treated with Ang-II for 24 h then removed it and transfected with the negative control inhibitor for 24 h.

Knockdown of TCF7 by siRNA

siRNA targeting TCF7 (siTCF7), and non-targeting control were synthesized by GenePharma. The transfection of siTCF7 was similar to that of siA02Rik/shA02Rik.

The sequences of siTCF7 were Forward: GGAAGAGAGGACAAGGAAUUT, Reverse: AUUCCUUGUCUCUCUCUUCCTT.

The sequences of negative control (N.C) were Forward: UGGAGCAA-GUUUGGCAGGAGCUAAU, Reverse: AAUAGCUCCUGCCAAACUUGCUCCA.

Cells were separated into four groups: (1) Control group; (2) Ang-II group; (3) Ang-II + siTCF7 group: cells were treated with Ang-II for 24 h then removed it and transfected with siTCF7 for 24 h; (4) Ang-II + N.C group: cells were treated with Ang-II for 24 h then removed it and transfected with the negative control for 24 h.

Luciferase reporter assays

A lncRNA02Rik fragment with miR-135a binding sites and TCF7 3'-UTRs was magnified by PCR. Briefly, HEK293 cells were incubated in 48-well culture plates. Lipofectamine 2000 (Invitrogen, Waltham, MA, USA) was used to transfect miR-135a-5p mimics at 10 pmol and luciferase reporter vectors at 40 ng/well. A dual-luciferase reporter assay kit (Promega) was used to detect firefly and renilla luciferase activity. Luciferase activity was normalized using firefly luciferase against renilla luciferase.

Adeno-associated virus-9-shA02Rik (AAV9-shA02Rik) infection in vivo

AAV9-shA02Rik and AAV9-shN.C were injected into mice via the tail vein (units: 1.2×10^{12} vg/mL, 100 µl, IBSBIO Tech). Sham group mice were treated similarly to TAC group mice but with 100 µl saline.

Mice were separated into four groups: (1) Sham group; (2) TAC + N.C group: saline was injected into mice on the second day after TAC for 3 weeks; (3) TAC + shA02Rik group: AAV9-shA02Rik was injected into mice on the second day after TAC for 3 weeks; (4) TAC + shN.C group: AAV9-shN.C was injected into mice on the second day after TAC for 3 weeks.

Statistical analysis

All statistical analysis was performed using SPSSv19.0 (SPSS Inc, Chicago, IL, USA), and data were presented as mean ± SD. The Student's *t*-test was used to compare differences between two groups. A one-way ANOVA was used to compare differences among groups. If the ANOVA was significant, SNK-*q* was used to evaluate the statistical significance of differences between the two groups. *P* < 0.05 was considered to be statistically significant.

DATA AVAILABILITY

The datasets used and analyzed during the current study are available from the corresponding author on reasonable request.

REFERENCES

- Komuro I, Yazaki Y. Control of cardiac gene expression by mechanical stress. *Annu. Rev. Physiol.* 1993;55:55–75.
- Gallagher J, James S, Keane C, Fitzgerald A, Travers B, Quigley E, et al. Heart failure virtual consultation: bridging the gap of heart failure care in the community-A mixed-methods evaluation. *ESC Heart Fail.* 2017;4:252–8.
- Ritterhoff J, Young S, Villet O, Shao D, Neto FC, Bettcher LF, et al. Metabolic remodeling promotes cardiac hypertrophy by directing glucose to aspartate biosynthesis. *Circulation Res.* 2019;126:182–96.
- Recamonde-Mendoza M, Werhli AV, Biolo A. Systems biology approach identifies key regulators and the interplay between miRNAs and transcription factors for pathological cardiac hypertrophy. *Gene.* 2019;698:157–69.
- Sun Y, Fan W, Xue R, Dong B, Liang Z, Chen C, et al. Transcribed ultraconserved regions, Uc.323, ameliorates cardiac hypertrophy by regulating the transcription of CPT1b (Carnitine Palmitoyl transferase 1b). *Hypertension.* 2020;75:79–90.
- Moretto F, Wood NE, Kelly G, Doncic A, van Werven FJ. A regulatory circuit of two lncRNAs and a master regulator directs cell fate in yeast. *Nat. Commun.* 2018;9:780.
- Piccoli MT, Gupta SK, Viereck J, Foinquinos A, Samolovac S, Kramer FL, et al. Inhibition of the cardiac fibroblast-enriched lncRNA Meg3 prevents cardiac fibrosis and diastolic dysfunction. *Circulation Res.* 2017;121:575–83.
- Lv L, Li T, Li X, Xu C, Liu QJ, Jiang H, et al. The lncRNA Plscr4 controls cardiac hypertrophy by regulating miR-214. *Mol Ther Nucleic Acids.* 2017;10:387–97.
- Peng L, Jiang B, Yuan X, Qiu Y, Peng J, Huang Y, et al. Super-enhancer-associated long non-coding RNA HCCL5 is activated by ZEB1 and promotes the malignancy of hepatocellular carcinoma. *Cancer Res.* 2018;79:572–84.

10. Zhao Y, Chu Y, Sun J, Song R, Li Y, Xu F. LncRNA GAS8-AS inhibits colorectal cancer (CRC) cell proliferation by downregulating lncRNA AFAP1-AS1. *Gene*. 2019;710:140–4.
11. Sun M, Nie F, Wang Y, Zhang Z, Hou J, He D. LncRNA HOXA11-AS promotes proliferation and invasion of gastric cancer by scaffolding the chromatin modification factors PRC2, LSD1, and DNMT1. *Cancer Res*. 2016;76:6299–310.
12. Pan W, Zhou L, Ge M, Zhang B, Yang X, Xiong X, et al. Whole exome sequencing identifies lncRNA GAS8-AS1 and LPAR4 as novel papillary thyroid carcinoma driver alternations. *Hum. Mol. Genet*. 2016;25:1875–84.
13. Gu J, Wang Y, Wang X, Zhou D, Shao C, Zhou M, et al. Downregulation of lncRNA GAS5 confers tamoxifen resistance by activating miR-222 in breast cancer. *Cancer Lett*. 2018;434:1–10.
14. Liu T, Liu S, Xu Y, Shu R, Wang F, Chen C, et al. Circular RNA-ZFR inhibited cell proliferation and promoted apoptosis in gastric cancer by sponging miR-130a/miR-107 and modulating PTEN. *Cancer Research*. 2018;50:1396–417.
15. Yang C, Yuan W, Yang X, Li P, Wang J, Han J, et al. Circular RNA circ-ITCH inhibits bladder cancer progression by sponging miR-17/miR-224 and regulating p21, PTEN expression. *Mol Cancer*. 2018;17:19.
16. Mateescu B, Batista L, Cardon M, Grusso T, de Feraudy Y, Mariani O, et al. MiR-141 and miR-200a act on ovarian tumorigenesis by controlling oxidative stress response. *Nat Med*. 2011;17:1627–35.
17. Sassi Y, Avramopoulos P, Ramanujam D, Grüter L, Werfel S, Giosele S, et al. Cardiac myocyte miR-29 promotes pathological remodeling of the heart by activating Wnt signaling. *Nat Commun*. 2017;8:1614.
18. Zhu HJ, Wang DG, Yan J, Xu J. Up-regulation of microRNA-135a protects against myocardial ischemia/reperfusion injury by decreasing TXNIP expression in diabetic mice. *Am J Transl Res*. 2015;7:2661–71.
19. Qi H, Ren J, E M, Zhang Q, Cao Y, Ba L, et al. MiR-103 inhibiting cardiac hypertrophy through inactivation of myocardial cell autophagy via targeting TRPV3 channel in rat hearts. *J Cell Mol Med*. 2019;23:1926–39.
20. Yuan J, Chen H, Ge D, Xu Y, Xu H, Yang Y, et al. Mir-21 promotes cardiac fibrosis after myocardial infarction via targeting Smad7. *Cell Physiol Biochem*. 2017;42:2207–19.
21. Liang R, Liu Y. Tcf7l1 directly regulates cardiomyocyte differentiation in embryonic stem cells. *Stem Cell Res Ther*. 2018;9:267.
22. Hou N, Ye B, Li X, Margulies KB, Xu H, Wang X, et al. Transcription factor 7-like 2 mediates canonical Wnt/ β -catenin signaling and c-Myc upregulation in heart failure. *Circulation Heart Fail*. 2016;9:10. 1161.
23. Giuliodori A, Beffagna G, Marchetto G, Fornetto C, Vanzi F, Toppo S, et al. Desmoplakin-deficient AC8 zebrafish models is rescuable by genetic and pharmacological intervention. *Cardiovascular Res*. 2018;14:082–1097.
24. Działo E, Rudnik M, Koning R, Czepiel M, Tkacz K, Baj-Krzyworzeka, et al. WNT3a and WNT5a transported by exosomes activate WNT signaling pathways in human cardiac fibroblasts. *Int J Mol Sci*. 2019;20:1436.
25. Kaplan N, Wang W, Christiaen L. Initial characterization of Wnt-Tcf functions during Ciona heart development. *Developmental Biol*. 2019;448:199–209.
26. Nagel R, le Sage C, Diosdado B, van der Waal M, Oude Vrielink JA, Bolijn A, et al. Regulation of the adenomatous polyposis coli gene by the miR-135 family in colorectal cancer. *Cancer Res*. 2008;68:5795–802.
27. Zhang L, Cheng H, Yue Y, Li S, Zhang D, He R. H19 knockdown suppresses proliferation and induces apoptosis by regulating miR-148b/WNT/ β -catenin in ox-LDL-stimulated vascular smooth muscle cells. *J Biomed Sci*. 2018;25:11.
28. Song C, Qi H, Liu Y, Chen Y, Shi P, Zhang S, et al. Inhibition of lncRNA Gm15834 attenuates autophagy-mediated myocardial hypertrophy via the miR-30b-3p/ULK1 axis in mice. *Mol Ther*. 2020;29:1120–37.
29. Micheletti R, Plaisance I, Abraham BJ, Sarre A, Ting CC, Alexanian M, et al. The long noncoding RNA Wisper controls cardiac fibrosis and remodeling. *Sci Transl Med*. 2017;9:395.
30. Wang Z, Zhang XJ, Ji YX, Zhang P, Deng KQ, Gong J, et al. The long non-coding RNA Chaer defines an epigenetic checkpoint in cardiac hypertrophy. *Nat Med*. 2016;22:1131–9.
31. Chen Z, Yu C, Zhan L, Pan Y, Chen L, Sun C. LncRNA CRNDE promotes hepatic carcinoma cell proliferation, migration and invasion by suppressing miR-384. *Am J Cancer Res*. 2016;6:2299–309.
32. Wang K, Liu CY, Zhou LY, Wang JX, Wang M, Zhao B, et al. APF lncRNA regulates autophagy and myocardial infarction by targeting miR-188-3p. *Nat Commun*. 2015;6:6779.
33. Huang Z-W, Tian L-H, Yang B, Guo R-M. Long noncoding RNA H19 acts as a competing endogenous RNA to mediate CTGF expression by sponging miR-455 in cardiac fibrosis. *DNA Cell Biol*. 2017;36:759–66.
34. Li Z, Liu L, Hou N, Song Y, An X, Zhang Y, et al. miR-199-sponge transgenic mice develop physiological cardiac hypertrophy. *Cardiovascular Res*. 2016;10:258–67.
35. Liang H, Pan Z, Zhao X, Liu L, Sun J, Su X, et al. LncRNA PFL contributes to cardiac fibrosis by acting as a competing endogenous RNA of let-7d. *Theranostics*. 2018;8:1180–94.
36. Ehler E, Moore-Morris T, Lange S. Isolation and culture of neonatal mouse cardiomyocytes. *J Vis Exp*. 2013;79:50154.
37. Louch WE, Sheehan KA, Wolska BM. Methods in cardiomyocyte isolation, culture, and gene transfer. *J Mol Cell Cardiol*. 2011;51:288–98.
38. Chen Y, Wang L, Huang S, Ke J, Wang Q, Zhou Z, et al. Lutein attenuates angiotensin II-induced cardiac remodeling by inhibiting AP-1/L-11 signaling. *Redox Biol*. 2021;44:102020.
39. Lim TB, Aliwarga E, Luu TDA, Li YP, Ng SL, Annadoray L, et al. Targeting the highly abundant circular RNA circSlc8a1 in cardiomyocytes attenuates pressure overload induced hypertrophy. *Cardiovascular Res*. 2019;115:1998–2007.

AUTHOR CONTRIBUTIONS

Conceived and designed the experiments: H.S. Performed the experiments: J.R., H.Q., C.S., L.B., R.L., X.F., L.W., M.Z., and Y.X. Analyzed the data: J.R. and H.Q. Wrote the paper: J.R., H.Q., and H.S.

FUNDING

This study was supported by the National Natural Science Foundation of China (81872856 and 82173810).

COMPETING INTERESTS

The authors declare no competing interests.

ADDITIONAL INFORMATION

Supplementary information The online version contains supplementary material available at <https://doi.org/10.1038/s41420-021-00775-8>.

Correspondence and requests for materials should be addressed to Hongli Sun.

Reprints and permission information is available at <http://www.nature.com/reprints>

Publisher's note Springer Nature remains neutral with regard to jurisdictional claims in published maps and institutional affiliations.



Open Access This article is licensed under a Creative Commons Attribution 4.0 International License, which permits use, sharing, adaptation, distribution and reproduction in any medium or format, as long as you give appropriate credit to the original author(s) and the source, provide a link to the Creative Commons license, and indicate if changes were made. The images or other third party material in this article are included in the article's Creative Commons license, unless indicated otherwise in a credit line to the material. If material is not included in the article's Creative Commons license and your intended use is not permitted by statutory regulation or exceeds the permitted use, you will need to obtain permission directly from the copyright holder. To view a copy of this license, visit <http://creativecommons.org/licenses/by/4.0/>.

© The Author(s) 2021